NUMERICAL MODEL OF THE LHP FOR THE THERMAL CONTROL OF THE CRYOMAGNET AVIONIC BOX (CAB) MOUNTED ON THE AMS-02 EXPERIMENT

Stefano Zinna[1], Marco Marengo[2], Marco Molina[3]
[1]UNIHEAT s. r. l,
viale Marconi 5, 24044 Dalmine (BG), Italy,
Tel. +39 3315714238; stefano.zinna@uniheat.it
[2]University of Bergamo, Microfluidic Lab
viale Marconi 5, 24044 Dalmine (BG), Italy
[3]Carlo Gavazzi Space
Via Gallarate 150, 20151 Milano, Italy

Abstract

AMS-02 is a space borne magnetic spectrometer designed to measure the composition of Cosmic Rays near Earth by using a superconducting magnet to bend the particle trajectory. Before starting the AMS-02 experiment is it necessary to charge the magnet. This will be done by the Cryomagnet Avionics Box (CAB), which is mounted to the primary structure of AMS-02. A LHP system is used for the CAB thermal control. In this paper the LHP model first designed in 2006 for the AMS-02 experiments is described using a numerical scheme for the lumped parameters thermal analysis of SINDA/FLUINT . By this model the temperature requirements for the CAB have been tested. Finally a sensitivity and a parametric analysis have been carried out to study the running time and the solution accuracy. Some design issues appeared to be critical and presently, starting from such results, the LHP system has been revised and a new model is under consideration.

KEYWORDS

Heat transfer, Space thermal control, LHP, AMS

INTRODUCTION

The international Alpha Magnetic Spectrometer experiment (AMS) is a particle detector for high energy cosmic rays. The scientific goal is to detect anti-matter, dark matter and dark energy. For this reason several detectors and sub-detectors operate in a magnetic field, which is generated by a super-conducting Helium-cooled magnet.

The experiment is designated AMS-02, since it is an improved version of AMS-01 flown on the Shuttle mission STS-91. AMS-02 is planned for a three to five years mission as attached payload on the ISS (Fig. 1). Before starting the AMS-02 experiment, the magnet will be charged by the Cryomagnet Avionics Box (CAB) which is the electronics unit for the power supply and control of the magnet. The CAB is mounted to the primary structure of AMS (called USS), on the WAKE side of the experiment.

Two sets of LHPs are implemented for the CAB thermal control, an upper and a lower one, both sunk to the WAKE radiator of AMS-02. The most dissipating items during magnet charge are six CCS (Constant Current Source) converter modules, located in the upper part of the CAB: for the thermal design it is preferable to have the LHP evaporators footprint as close as possible to the CCS, although some of them are not accessible, being located underneath the mechanical fixation to the USS.

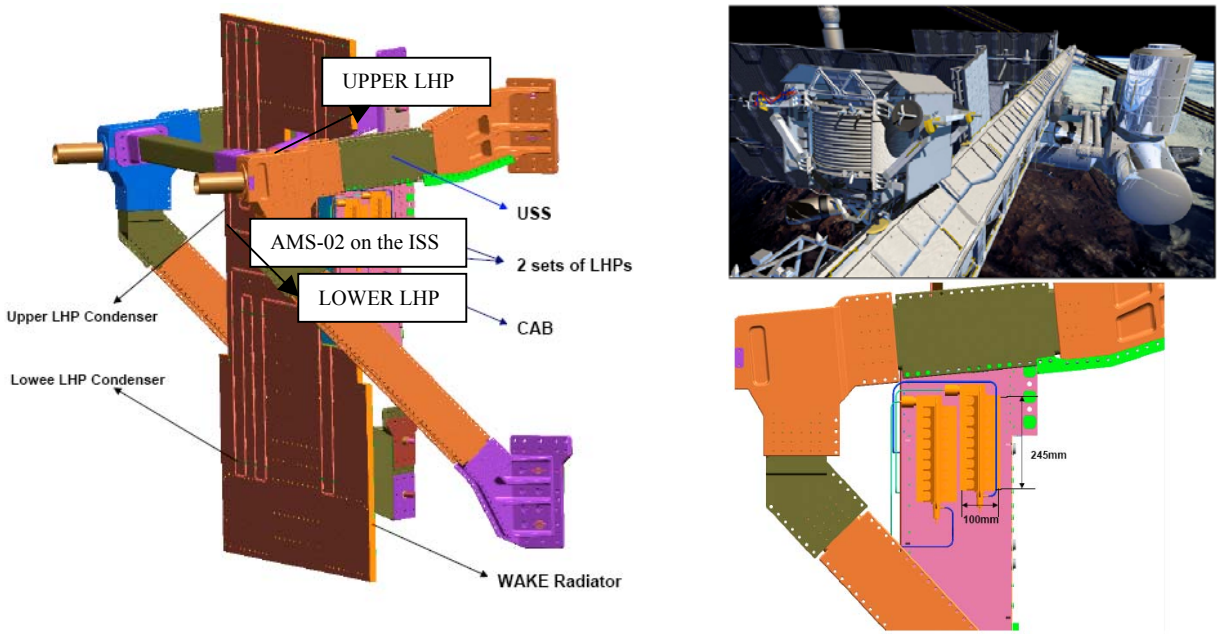

Fig. 1. CAB and 2 sets of LHPs, the USS and the WAKE Main radiator

The nominal operation of the CAB is a typical command-and-control function of the cryomagnet system. The “Ramp up” mode is the one which allows charging the magnet up to 460 A of current. In this latter phase, the dissipation of the CAB can arrive up to 750 W (Fig. 2). This power could further increases under the failure of one of the CCS converters. In this case the remaining 5 CCS should assure the charging of the magnet, dissipating each a bigger power than the nominal operation and reaching together up to 827 W.

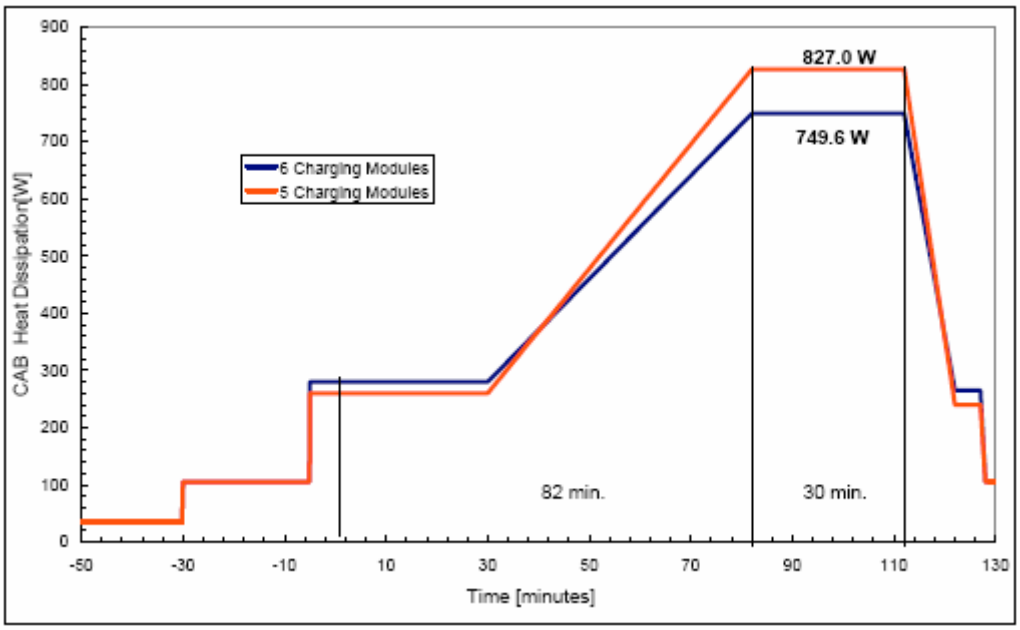

Fig. 2. CAB power profile during charging the magnet, original charge profile considered in years 2004–2007

Another typical operational mode is characterizing by steady state power supplied to the CAB. In this case the total dissipation is a minimum of 35.5 W, that we will considered combined to a cold environment (i.e. cold orbital sink temperatures and solar fluxes towards the radiator) and 105.3 W for an hot environment.

The LHPs, together with the other CAB thermal control means (body mounted radiator of silvered Teflon and conductive interface to the USS), are required to guarantee CAB operation even in the failure of one of the LHPs. The CAB thermal requirements to be verified at the skin level of the unit (base-plate and rear side facing wake) are driven by the internal temperatures and are defined as the temperatures at which the maximum working limit of the electronics components are reached. The goal of the CAB-LHP system is to keep component temperatures between -25 °C and the maximum temperature limits as showed table 1 for RAMP-UP and table 2 for steady state mode.

Since the research was devoted to understand the general behaviour of the system, in order to find possible hints with a reasonable computing time, in this paper the failure of only one of the LHPs mounted on the CAB base plate is considered for every operational mode. Indeed, usually the bottleneck in the running time is the fluid part so that to include two LHPs and consequently two fluid lines could bring to a big time consuming model. After, the failure of one LHP represents one of the most critical operational mode, hence to satisfy the requirements under this case is a guarantee for the other conditions. Vice-versa the limits overcoming should be carefully considered by different configurations during the magnet charging (i.e. by using 2 LHPs).

The lumped parameter code SINDA/FLUINT is used to model all the elements of the LHP. Because not all the LHP geometrical data were fixed from the beginning, a sensitivity analysis has been carried out in order to control possible important variations of the thermal behaviour changing the designed LHP parameters. After simulating a first LHP model, further analyses have been performed to check the error range and to improve the running time.

Table 1. CAB base-plate and rear side (wake radiator) temperature design requirements (in °C) for RAMP-UP under the failure of 1 LHP

Base Plate node ID	201	202	203	204	205	206	207	208	209	210	211	212	213	214	215	216	217	218	219
T limit [°C]	71	71	70	69	68	68	68	68	69	72	74	75	76	76	77	77	77	77	77
Rear Side node ID	301	302	303	304	305	306	307	308	309	310	311	312	313	314	315	316	317	318	319
T limit [°C]	71	71	71	71	71	71	72	72	73	73	73	73	73	73	73	73	73	73	73

Table 2. CAB base-plate and rear side (wake radiator) temperature design requirements (in °C) for steady state operation under the failure of 1 LHP

Base Plate node ID	201	202	203	204	205	206	207	208	209	210	211	212	213	214	215	216	217	218
T limit [°C]	72	73	72	67	65	63	58	55	55	57	59	60	60	60	61	61	61	61
Rear Side node ID	301	302	303	304	305	306	307	308	309	310	311	312	313	314	315	316	317	318
T limit [°C]	67	67	67	66	65	64	63	62	61	60	60	61	61	61	61	61	61	61

SINDA/FLUINT LHP MODEL

In the following paragraphs the SINDA/FLUINT model will be described. As the evaporator and the condenser are the most important LHP sections, only these parts will be then characterized. As already stated, since the CAB TCS design is in-progress and some geometric characteristics are expected to be changed a range of many thermal parameters has been defined rather than a single precise value. Then, these ranges have been inserted in the SINDA/FLUINT model and the LHP working has been tested with its most common limits. Hence only the geometric characteristics that satisfy these limits has been considered for the RAMP-UP and Steady state cases.

Evaporator

In SINDA/FLUINT the evaporator scheme is constituted by nodes representing the thermal and fluid volumes being inside it. Majority of the heat input goes into vaporizing liquid or it is leaked into the compensation chamber. The ratio between those two heat links depends on the ratio between their corresponding conductances: $\mathbf{U_{Wb} = U_W/G_{back}}$. The other heat contribution coming away from the evaporator wall transfers only a little portion of the overall power, hence this ratio assumes a crucial importance in the LHP performance.

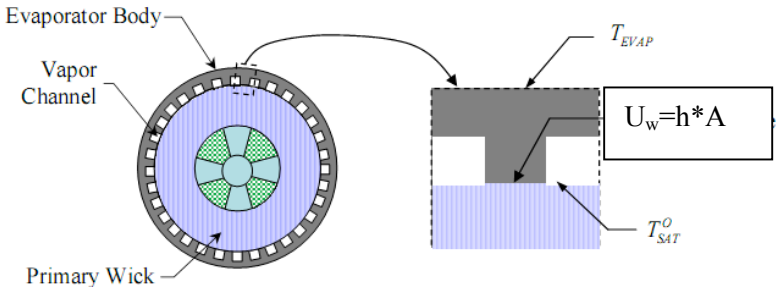

Fig. 3. Magnified view of the heating surface in the evaporator

The heat transfer in the wick (Fig. 3) is much more complicated then the boiling heat transfer for plain surfaces. Therefore, most of the related studies are based on experimental data. Po-Ya Abel Chuang [2] got experimental results of the heat transfer coefficients as a function of heat flux when the LHP is operated at zero elevation. The data are achieved for a LHP with Nickel powder wick and Ammonia as working fluid.

Other experimental data are reported in the work of Michelle L. Parker [3] for the combination Nickel powder wick and Ammonia. Depending on his analysis the Uw is set to 5000 W/(m^2·K) in order to allow good correlation data. This value falls in the regime suggested in the literature [2] (5000-10000 W/(m^2·K)) that will be used as a reasonable range in the CAB LHP model.

The back conduction links the outer surface of the wick to the inner surface which is essentially part of the compensation chamber. Because its value is strongly connected to Uw, the same scheme used in Michelle L. Parker work has been implemented here. It has been derived by Fershtater [3]:

$$G_{back} = \dot{m} c_{pl} \left[\frac{(R_i / R_o)^{\eta}}{1 - (R_i / R_o)^{\eta}} \right], \qquad \eta = \frac{\dot{m} c_{pl}}{2\pi k_{eff} L}, \tag{1}$$

where R_0 and R_i are the external and internal wick radius, L is the length of the compensation chamber. The effective conductivity of the wick is obtained from Chaudary and Bhandari model:

$$k_{eff} = k_{\max}^{n} k_{\min}^{1-n} \tag{2}$$

where: n = 0.42 (Michelle L. Parker),

$k_{\max} = \phi k_f + (1-\phi) k_s$ (parallel paths),

$k_{\min} = (k_s k_f) / (\phi k_s + (1-\phi) k_f)$ (paths in series).

K_s = conductivity of the solid,
K_f = conductivity of the fluid,
Φ = porosity.

Condenser

The condenser is attached to the Wake radiator as shown in the next picture.

The condenser is subdivided into 23 nodes (ID from 301 to 323). As it is visible in Fig. 4 most of the nodes are located in the upper part. The lay-out shown in the figure results from the following considerations:

- The wake radiator has embedded heat pipes in order to spread the heat all along the surface. The heat pipes are laid vertically hence the temperature drop in this direction is minimal. As a result the condenser nodes are spread in the horizontal direction.
- Most of the nodes is located where the lower condenser section (with the incoming two-phase flow) is near the upper part (with the outgoing subcooled fluid) in order to account for the resultant heat transfer.
- Most of the nodes are located close to the initial and final section of the condenser in order to account for the big heat transfer dues to the great temperature difference between these two parts.

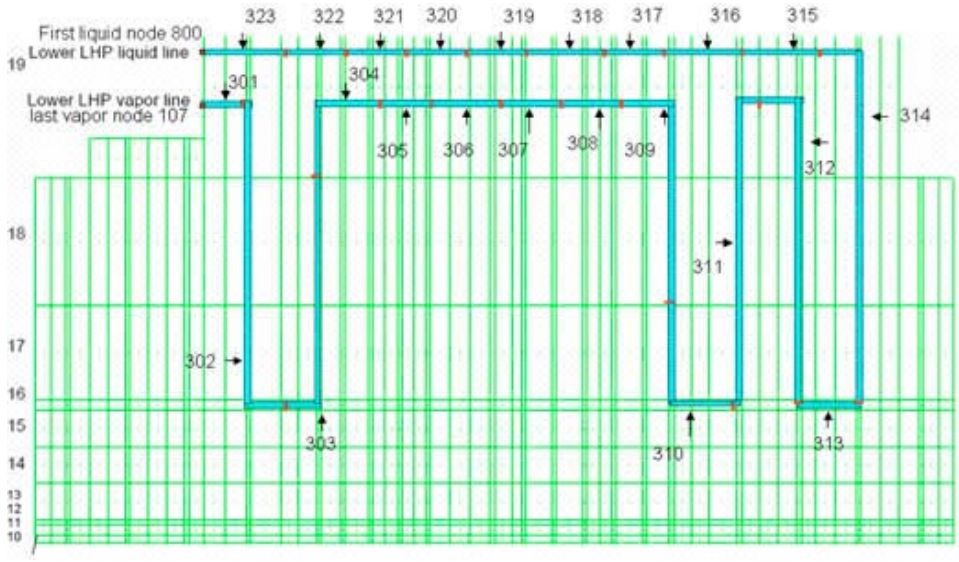

Fig. 4. Condenser nodes attached to the radiator

Shear-driven film condensation within an externally cooled constant diameter tube can be considered as a form of film condensation, hence this kind of process is considered to happen inside the LHP condenser. Vapour enters the tube at saturation conditions, condenses on the cool wall, wets the surface, and form an annular liquid film. In particular the Shah correlation will be the input in the SINDA/FLUINT model [1]:

$$Nu = Nu_{lo}\left[(1-x)^{0,8} + \frac{3{,}8x^{0,76}(1-x)^{0,04}}{p_r^{0,38}}\right] \qquad \begin{aligned} p_r &= P/P_C \\ Nu_{lo} &= 0{,}023\,\mathrm{Re}_{lo}^{0,8}\cdot \mathrm{Pr}_l^{0,4} \end{aligned} \tag{3}$$

where P_C is the critical pressure, Pr_r is the Prandtl number at bulk liquid temperature. Such empirical correlation is oversimplified, but it provides a robust estimation and is valid also for the transition between the single phase and the two-phase mode.

LHP Design

First an overview of the common LHP working limits used in this analysis is introduced.

The evaporator is the most important section for the LHP working. Heat input from a heat source conducts through the capillary pump body to vaporize liquid in both sides of the primary wick. As settled from Hoang et al. [5] for a common LHP, majority of the heat input (>90 % of the overall) goes into vaporizing liquid on the outer surface of the primary wick. Hence a value bigger than 90 % is assumed here (**first limit**).

The compensation chamber must satisfy the minimum volume requirement [6]. The compensation chamber volume must be able to accommodate at least the liquid volume difference (and density changes) between the hot case and the cold case of the loop operation. The LHP is usually charged in a way that some liquid is left in the compensation chamber when the rest of the loop is completely flooded under the cold case (**second limit**), and some vapour space is available in the compensation chamber when the condenser is fully used under the hot case (**third limit**).

Moreover the fluid charge must be checked against the upper limit allowed by the loop (**fourth limit**). An upper limit exists because the loop must be able to contain all the liquid volume at the maximum non-operating temperature in order to prevent bursting due to the hydrostatic pressure.

Finally some relationship will be considered as reasonable for the wick properties (**fifth limit** [6], table 3).

Table. 3 Characteristics of capillary structures

Material	Porosity, %	Effective pore radius, μm	Permeability, $x10^{13}$, m^2	Thermal conductivity, W/(m·K)
Nickel	60-75	0.7-10	0.2-20	5-10

Now the Newton-Rapshon iteration procedure has been run to look for the geometric characteristics that satisfy the working limits introduced above. It is important to highlight that different sets of the geometric parameters could result as "good" for the LHP thermal behaviour, i.e. there are multiple parametric solutions for the "working limits" analysis.

Every parameter set may have a different U_w/G_{back} ratio even if the ratio always falls into a reasonable range:

$$10 < (U_W / G_{back}) < 13 . \tag{4}$$

Therefore, an averaged value equal to 11.5 is used in the present CAB LHP model. Further information about the temperature error will be discussed in the parametric analysis.

LHP MODEL SIMULATIONS

During the steady state mode the CAB temperatures fall into the range shown in the table 4. As shown the temperature requirements are satisfied, both for the lower limit (-25 °C) and for the upper one (table 2).

Table. 4 Steady State maximum and minimum temperatures

Temperature, °C	Rear side, HOT	Base-plate, HOT	Rear side, COLD	Base-plate, COLD
T min	50.8	48.8	-23.5	-22.47
T max	55.3	64	-21.8	-19

The following figures show the CAB base-plate (Fig. 5) and the Rear side temperatures together with the temperature limits (horizontal lines) during the ramp-up when the magnet is charged.

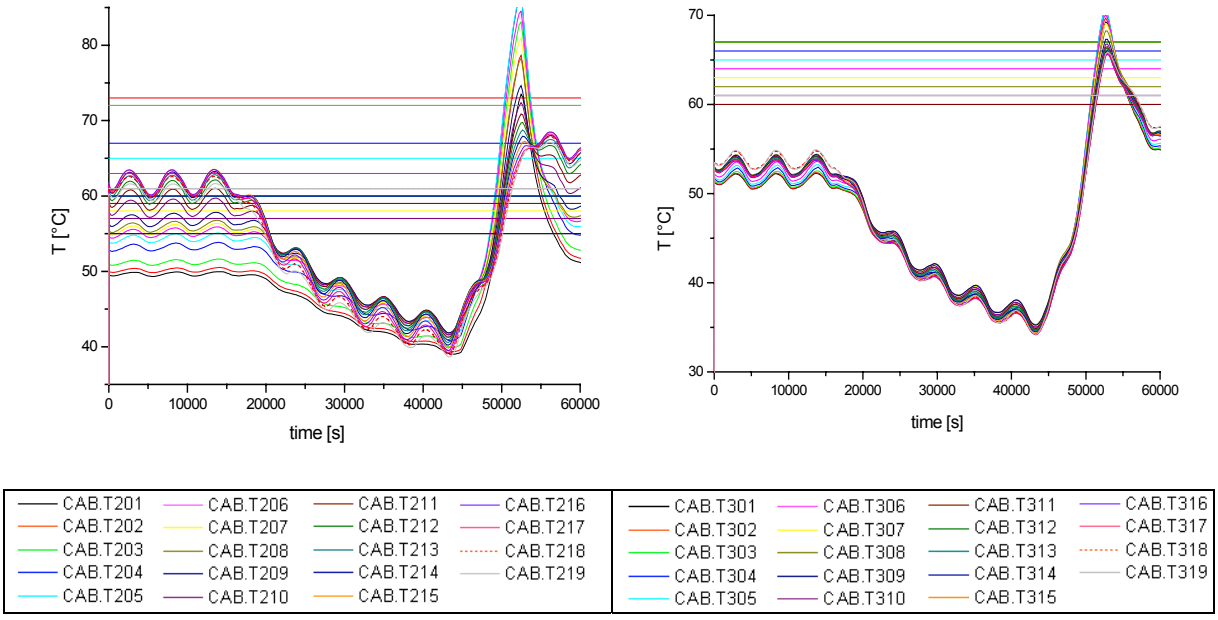

Fig. 5. CAB base-plate node temperatures & requirements on the left, Rear side node temperatures & requirements on the right, RAMP-UP

It is clear that both in CAB base plate and in the rear side the temperature limits are overcome during the power peak of the ramp profile (between 50000 and 60000 s). The Node 207 and 208 show the highest overruns from the limits for the CAB (about 22 °C) and Node 310 for the Rear side (about 6 °C). Further comments will be found in the next paragraph.

These simulations have been obtained by nominal values for the SINDA/FLUINT running parameters that drive the accuracy in the temperature calculations. As a result of this setting the model run is slow and the resultant RAMP-UP running time is about 1 week. Therefore a sensitivity analysis has been carried out (next paragraph) to look for the set of the running parameters that both decrease the running time and preserve the desired accuracy.

RUN TIME ANALYSIS AND ACCURACY OF THE SIMULATIONS

First a sensitivity analysis is carried out with the goal to modify the SINDA running parameters in order to find a faster SINDA model which guarantees the desired accuracy. Then a parametric analysis is proposed in order to test the temperature inaccuracies due to the geometric uncertainty as previously explained.

Sensitivity Analysis (SA)

The SINDA solver performs a transient thermal analysis by implicit forward-backward differencing. There is no upper bound on the time step due to stability considerations for this implicit method. However, the user must realize that as the time step becomes larger, so will the error imparted to the resulting temperatures. Automatic time step predictions to control this error are available by setting the vector of the running parameters (***k***, Table 5).

Table 5. Parameters tested

K_1	Maximum temperature change allowed for convergence of non-inertial thermal nodes
K_2	Maximum temperature change allowed for convergence of inertial thermal nodes
K_3	Fractional change allowed in fluid key variables (temperatures, flow rates, pressures etc..).

The sensitivity analysis has been run to test the influence of these parameters on the vector of the variables (***y***): running time and accuracy in the solutions. Their effect is considered not influenced by the boundary conditions. This simplification let us to use a time-independent system to characterize the sensitivity analysis, which is then reduced to find either a minimum or the zero-value of a "objective"-function ***f***:

$$0 = \boldsymbol{f}(\boldsymbol{y}, \boldsymbol{k}). \tag{1}$$

Local SA is usually carried out by computing partial derivatives of the output variables with respect to the input factors. The analysis is achieved under the following assumptions:

- parameter changes within the round-off error (2.0E-13 for double precision) will be neglected;
- The influence of the parameters is additive;
- The boundary conditions are fixed to the HOT case.

The relative change in the compensation chamber temperature is used to quantify the accuracy error:

$$\frac{\boldsymbol{T}^* - \boldsymbol{T}_0}{\boldsymbol{T} - \boldsymbol{T}_0}, \tag{2}$$

where T* is the temperature calculated by changing the parameter, T_0 is the steady state temperature and T is the nominal calculated temperature.

The table 6 shows the results, obtained by Newton-Raphson method, if a 5 % range is considered as admissible. It is shown a very small improving in the running time compared with the accuracy lost:

the maximum time saved is 0.14 % when a temperature error equal to 1 °C is considered reasonable. The same result is noticed for error up to 5 °C, so that the sensitivity to the parameters is negligible in the range between 1 and 5 degree.

Obviously, the computational time could be shorter if the parameters would be considered acceptable over 5 % of the nominal value. However there is no guarantee about their reliability (namely, linearity) in these ranges. Finally the default (nominal) parameters are used for the simulations.

Table 6. Results, range equal to 5% of the default value

Accuracy error (based on 273K)	Running time saved %	0,0095< K_1<0,0105	0,0095<K_2<0,0105	0,095< K_3<0,105
1–5 °C	0.14	0.0105	0.0105	0.0105

Parametric analysis

As it has been explained, not all the geometrical data in the LHP has been fixed. Consequently the ratio between the heat transfer coefficients in the evaporator (U_{wb}), that is function of the evaporator geometric characteristics, fall into a reasonable range. A parametric analysis have been run to test the temperature error due to such uncertainties. Also the power coming in the LHP evaporator (Q) and the orbital environment (HOT and COLD) have been included in this analysis as parameters.

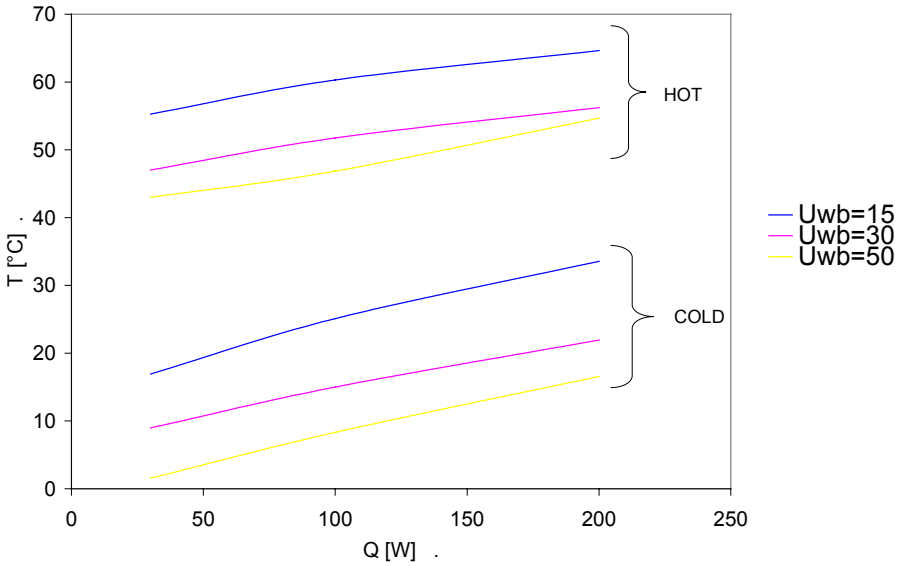

Fig. 6. Parametric analysis

The Fig. 6 shows the variation of the compensation chamber temperature with the increase of the input power in stationary conditions varying the ratio Uwb. The result proves that HOT and COLD environmental show similar trend at two different temperature levels. Both cases has linear dependence on the power and the LHP temperature decrease for higher U_{wb} values. Eventually the HOT case for U_{wb} = 30 shows a slight deviation when high power is considered.

Now, following the parametric analysis, it is possible to quantify the temperature errors due to the uncertainty in the U_{wb} value. The incremental ratio (between the temperature and U_{wb}) is estimated by:

$$\Delta T_{U_{wb}} = \frac{\Delta T}{\Delta U_{wb}} = \frac{T_{Uwb1} - T_{Uwb2}}{U_{wb1} - U_{wb2}} \tag{3}$$

where T_{Uwb} is the compensation chamber temperature calculated for U_{wb}.

It is possible to settle that an uncertainty in the U_{wb} value equal to 3 (from 10 to 13) brings to an uncertainty in the temperatures equal to 1.02°C and 1.28°C under hot and cold conditions respectively.

The little amount of this deviation has no important influence on the results so that the temperature overcome shown in Fig. 5 can be confirmed.

CONCLUSION

The present paper analyses the running conditions for the Cryomagnet Avionic Box (CAB) on the International Space Station. Three operational modes are analyzed for the CAB: HOT Steady state, COLD Steady state and RAMP-UP and the failure of only one LHP is considered.

The LHP model for the simulation has been realized by using the lumped parameter code SINDA/FLUINT. The results show that the steady state mode satisfies the temperature requirements while during the RAMP-UP these limits are exceeded, unless suitable relaxation of the ramp-up parameters will be done.

The paper shows that even if at the beginning of the design activity and despite the lack of values for some LHP parameters, an accurate sensitivity analysis together with the right choice of the physical parameters is able to produce robust results with a possible temperature variation, for the considered range of the boundary conditions, equal to maximum 1.28 K (in cold conditions). Therefore the conclusions about the LHP temperatures can be confirmed even if some physical and geometrical parameters are not well defined and still to be completely designed.

At the end, considering the present outcome, corrective actions to overcome this over-temperature problem have been recently implemented:

- a limitation to 400 A to the magnet charge, requiring only 15 minutes of stabilization instead of 30 as simulated so far, driven by safety and system level considerations
- the elimination of the requirement to make the ramp possible with 1 LHP only. It shall be possible to ramp-up the magnet in hot orbits with both LHPs working.
- The relaxation about operations in the hottest environment: due to ISS orbit precession it is possible to wait less than 10 days to restore thermally benign conditions for having a successful ramp-up.

With these requirements relaxation the complete feasibility of the project has been assessed.

References

1. Basil N. Antar and Vappu S. Nuotio-Antar. *Fundamentals of Low Gravity Fluid Dynamics and Heat Transfer*. CRC Press, Boca Raton, Florida, 1993.
2. Po-Ya Abel Chuang, *An improved steady-state model of loop heat pipes on experimental and theoretical analyses*. PhD thesis, University of Pennsylvania, Pennsylvania, 2003.
3. Michelle L. Parker, *Modeling of Loop Heat Pipes with Applications to Spacecraft Thermal Control*, Phd Thesis, University of Pennsylvania, Pennsylvania, 2000.
4. Liao, Q. and Zhao, T. S., Evaporative Heat Transfer in a Capillary Structure Heated by a Grooved Block // *J. of Thermophysics and Heat Transfer*, 1999, Vol. 13, No. 1, pp. 126-133.
5. Triem T. Hoang, Jentung Ku, Heat and Mass transfer in loop heat pipes // *Proceedings of 2003 ASME Summer Heat Transfer Conference*, 2003.
6. Operating Characteristics of Loop Heat Pipes Jentung Ku // *29th International Conference on Environmental System*, 1999, Denver, Colorado.
7. Yu.F. Maydanik, Loop heat pipes // *Applied Thermal Engineering,* 2005, Vol 25, pp. 635–657.
8. Saltelli A., K. Chan, E.M. Scott. *Sensitivity Analysis*, John Wiley & Sons Ltd, 2000, England.